ANTIMICROBIAL AGENTS AND CHEMOTHERAPY, Mar. 2007, p. 982–990 Vol. 51, No. 3
0066-4804/07/$08.00+0 doi:10.1128/AAC.01510-06

Reduced Susceptibility to Polyenes Associated with a Missense Mutation in the *ERG6* Gene in a Clinical Isolate of *Candida glabrata* with Pseudohyphal Growth[▽]

Patrick Vandeputte,[1]* Guy Tronchin,[1] Thierry Bergès,[2] Christophe Hennequin,[3] Dominique Chabasse,[1] and Jean-Philippe Bouchara[1]

Groupe d'Etude des Interactions Hôte-Parasite, UPRES-EA 3142, Laboratoire de Parasitologie-Mycologie, Centre Hospitalier Universitaire, 49933 Angers Cedex 9,[1] Laboratoire de Génétique de la Levure, CNRS UMR 6161, Faculté des Sciences, 86022 Poitiers Cedex,[2] and Laboratoire de Parasitologie-Mycologie, Hôpital Tenon, 75970 Paris Cedex 20,[3] France

Received 30 November 2006/Accepted 2 December 2006

Little information is available about the molecular mechanisms responsible for polyene resistance in pathogenic yeasts. A clinical isolate of *Candida glabrata* with a poor susceptibility to polyenes, as determined by disk diffusion method and confirmed by determination of MIC, was recovered from a patient treated with amphotericin B. Quantitative analysis of sterols revealed a lack of ergosterol and an accumulation of late sterol intermediates, suggesting a defect in the final steps of the ergosterol pathway. Sequencing of Cg*ERG11*, Cg*ERG6*, Cg*ERG5*, and Cg*ERG4* genes revealed exclusively a unique missense mutation in Cg*ERG6* leading to the substitution of a cysteine by a phenylalanine in the corresponding protein. In addition, real-time reverse transcription-PCR demonstrated an overexpression of genes encoding enzymes involved in late steps of the ergosterol pathway. Moreover, this isolate exhibited a pseudohyphal growth whatever the culture medium used, and ultrastructural changes of the cell wall of blastoconidia were seen consisting in a thinner inner layer. Cell wall alterations were also suggested by the higher susceptibility of growing cells to Calcofluor white. Additionally, complementation of this isolate with a wild-type copy of the Cg*ERG6* gene restored susceptibility to polyenes and a classical morphology. Together, these results demonstrated that mutation in the Cg*ERG6* gene may lead to a reduced susceptibility to polyenes and to a pseudohyphal growth due to the subsequent changes in sterol content of the plasma membrane.

Among pathogenic yeast species, *Candida glabrata*, which accounts for 5% to 40% of all yeast isolates depending on the studies (16), ranks second in all clinical forms of candidiasis today. This opportunistic pathogen is critical in immunocompromised patients, like those receiving cytotoxic drugs for bone marrow or organ transplantation as well as patients infected by the human immunodeficiency virus (21, 31). Moreover, due to its poor susceptibility to current antifungals and to the emergence of resistance (26, 29), there is growing concern for the treatment of infections caused by *C. glabrata*.

To fight these infections, four classes of antifungal molecules are now available, e.g., polyenes, pyrimidin analogs, azoles, and echinocandins. Amphotericin B and nystatin, the two major representatives of polyene molecules, destabilize the yeast membrane by their binding to ergosterol, which is the main sterol species of the plasma membrane in yeasts (10).

If resistance mechanisms to azole antifungals have been widely investigated, mechanisms of polyene resistance are poorly understood in clinical isolates, since resistance to these antifungals remains uncommon. Since ergosterol is the main target of polyenes, resistance may arise from a decrease in ergosterol content or from a complete lack of ergosterol in the plasma membrane as a consequence of mutations in genes encoding some of the enzymes involved in the ergosterol biosynthesis pathway (10). Mutations in several genes leading to polyene resistance, but permitting cell viability, have been described for *Candida lusitaniae* and *Candida albicans* (28, 42). Proteins encoded by these genes are usually involved in the last steps of the ergosterol pathway, and mutations in these genes lead to a decreased susceptibility to polyenes without destabilization of the plasma membrane. Polyene resistance is frequently associated with resistance to azoles (28). When cells lack ergosterol or when the ergosterol amount dramatically decreases, the role of the cytochrome P450 lanosterol 14 α-demethylase in membrane constitution is less important and azole drugs have a lower effect on cell viability and growth.

Among *Candida* species, *C. glabrata* is particular, as it is genetically closer to *Saccharomyces cerevisiae* than other *Candida* species. Moreover, like *S. cerevisiae*, *C. glabrata* cannot perform dimorphic transition from blastoconidia to hyphae or pseudohyphae under usual culture conditions (23). However, *C. glabrata* can produce pseudohyphae, as has been reported for both yeast species, in special culture conditions like nitrogen starvation (8) or in the presence of $CuSO_4$ (17). The recent recovery in our hospital laboratory of a clinical isolate of *C. glabrata* with a poor susceptibility to polyene drugs associated with a pseudohyphal growth led us to investigate the mechanisms responsible for its particular phenotype.

* Corresponding author. Mailing address: Groupe d'Etude des Interactions Hôte-Parasite, UPRES-EA 3142, Laboratoire de Parasitologie-Mycologie, Centre Hospitalier Universitaire, 4 rue Larrey, 49933 Angers Cedex 9, France. Phone: 33 02 41 35 34 72. Fax: 33 02 41 35 36 16. E-mail: patrick.vandeputte@etud.univ-angers.fr.

▽ Published ahead of print on 11 December 2006.

TABLE 1. Oligonucleotides used for gene sequencing and evaluation of gene expression

Gene name (gene product)	GenBank accession no.	Primer	Nucleotide sequence (5′–3′)	Nucleotide coordinates[a]
Cg*ERG4* (C-24[28] sterol reductase)	NC005967	ERG4-1F	CAACACAATAATCGGTGGGGT	44666–44686
		ERG4-1R	CAAGGATGTTACAATAATGCA	44082–44102
		ERG4-2F	CTCCAGTGATAAACATAAACG	44228–44248
		ERG4-2R	AAACACCTGGCAGAGTGTAA	43654–43673
		ERG4-3F[b]	TCATCGGCAAACTTTACCA	43794–43812
		ERG4-3R[b]	AGCCATATGTTTCATATTGCT	43333–43353
		ERG4-4F	TTGACTTGAAGATGTTCTTCG	43380–43400
		ERG4-4R	TGATCCATTGGAAGTGACCA	42895–42914
		ERG4-5F	TGTCTGGCGATAAGACTGTCA	42945–42965
		ERG4-5R	CCCATGAACCGTTTTTCCTT	42414–42433
Cg*ERG5* (C-22 sterol desaturase)	NC006036	ERG5-1F	TTGACTACCGTATCGGGGATT	765352–765372
		ERG5-1R	TGGCATTCATGCTCATATGC	765995–765814
		ERG5-2F[b]	TGCAATTGGGATACCCGATT	765699–765718
		ERG5-2R[b]	CCATCAATTCTTCCAAAGGAG	766301–766321
		ERG5-3F	AAAGCCCACACCGACTATAGA	766231–766251
		ERG5-3R	GCATCTTGAGAAGCGAACAA	766762–766781
		ERG5-4F	AACCGTACCGACGATGACTCT	766684–766704
		ERG5-4R	ACCGATCAAAGCAGTCATGGT	767215–767235
		ERG5-5F	TCCACACGTTTGTCTAGGTCA	767178–767198
		ERG5-5R	CTGGGAAAGATTTGCAATAGG	767510–767530
Cg*ERG6* (Δ[24] sterol C-methyltransferase)	NC006031	ERG6-1F	CGGCATTTGGATTTTCTCGT	444995–445014
		ERG6-1R	TCGGGAGAATTTCAATTCC	445490–445508
		ERG6-2F	CAGTTTATTGTGCTCTTGACG	445443–445463
		ERG6-2R	TGAATCTGGCGATGGTACG	445932–445949
		ERG6-3F[b]	GCATACATGGCCGGTATCAA	445862–445881
		ERG6-3R[b]	ACTTCCATTCACCGGTCAAT	446395–446414
		ERG6-4F	TTTGAAGAACGTCGGTTCG	446317–446336
		ERG6-4R	CATGTGGAATGAATTCAAGTG	446821–446841
Cg*ERG11* (lanosterol 14-α demethylase)	L40389	ERG11-1F	CTACAATCGAGTGAGCTTG	17–35
		ERG11-1R	GTAGAACACAAGTGGTGG	729–746
		ERG11-2F	GGTCGTTGAACTATTGGAG	584–602
		ERG11-2R	GGACCCAAGTAGACAGTC	863–880
		ERG11-3F[b]	CCATCACATGGCAATTGC	688–705
		ERG11-3R[b]	GGTCATCTTAGTACCATCC	1445–1463
		ERG11-4F	CGTGAGAAGAACGATATCC	1380–1398
		ERG11-4R	CACCTTCAGTTGGGTAAC	2047–2064
		ERG11-5F	CGCTTACTGTCAATTGGG	1991–2008
		ERG11-5R	GTCATATGCTTGCACTGC	2397–2414
Cg*ERG9* (squalene synthase)	AB009978	ERG9 F[b]	TGATTCTGAGGGCTTTGGA	725–743
		ERG9 R[b]	TACAATCGACACCCTTTTGG	1293–1312
Cg*ERG1* (squalene epoxydase)	AF006033	ERG1 F[b]	CGTTGCTTTTGTTCATGGTAG	1–21
		ERG1 R[b]	ATACCACCACCAGTTAGAGGG	589–609
Cg*ERG2* (C-8 sterol isomerase)	NC006035	ERG2 F[b]	TGTACTTGCCAAACACAACG	1142387–1142406
		ERG2 R[b]	ACAAATCCAAAGTGGAGGAGA	1142840–1142860
Cg*ERG3* (C-5 sterol desaturase)	L40390	ERG3 F[b]	AAGATTGCGCCTGTTGAGTT	615–634
		ERG3 R[b]	TACCACAGTCGGTGAAGAAGA	1129–1149
Cg*CDR1* (ABC transporter)	AF109723	CDR1 F[b]	GAAGTCTATGGAAGGTGC	1084–1101
		CDR1 R[b]	GTCTAGCGTAAGTCTCTC	1383–1400
Cg*CDR2* (ABC transporter)	AF251023	CDR2 F[b]	GTTGAGTACTGGCACAAC	362–379
		CDR2 R[b]	GATGGCAAAGAACATGGC	695–712
Cg*STE12* (MAP-activated transcription factor)	AJ515385	STE12 F[b]	AAGCTGTAACACATCTCATGC	855–875
		STE12 R[b]	AACAGGAGTCATATGCGAAG	1472–1491
Cg*ACT* (β actin)	AF069746	ACT F[b]	TATTGACAACGGTTCCGG	949–966
		ACT R[b]	TAGAAAGTGTGATGCCAG	1177–1194

[a] Nucleotide coordinates refer to the corresponding gene sequence in the GenBank database.
[b] Primers used for evaluation of gene expression.

MATERIALS AND METHODS

Yeast strains and culture conditions. This study was carried out using two. *C. glabrata* clinical isolates. The first one, designated 40400178, was recovered in the Laboratory of Parasitology and Mycology of Angers University Hospital in 2004 from a 75-year-old man hospitalized for an erysipelas of the left leg associated with a heel scab. Despite antibiotic treatment, he developed gangrene and his left leg was amputated in January 2004. From December 2003 to January 2004, he received amphotericin B (1 g per day orally) for stomatitis. At the end of December, he presented with a cutaneous rash and developed a fever at the beginning of January. Culture of a urine sample collected at this date revealed the exclusive growth of a yeast that was identified as *C. glabrata* using the ID32C test strip (Biomérieux, Marcy-l'Etoile, France). Antifungal susceptibility testing, performed using a Fungitest strip (Bio-Rad, Marnes-la-Vallée, France), revealed a low susceptibility to amphotericin B for this isolate. The patient died at the end of January 2004. Since no matched susceptible isolate was available for further study of antifungal resistance mechanisms, another clinical isolate, designated 90.1085 and already described in previous studies from our group (4, 5, 9), was used as a control.

The two clinical isolates were maintained by biweekly passages on yeast extract-peptone-glucose (YEPD) agar plates containing (in g/liter): yeast extract, 5;

peptone, 10; glucose, 20; chloramphenicol, 0.5; agar, 20. Both isolates were preserved by lyophilization and by freezing at −80°C in 20% (wt/vol) glycerol. In addition, they were deposited at the IHEM (Institute of Hygiene and Epidemiology, Mycology section) Culture Collection (Brussels, Belgium) and are publicly available under the accession numbers 21231 and 21229 (for 90.1085 and 40400178, respectively).

Antifungal susceptibility testing. Susceptibility to polyene and azole drugs was determined by a disk diffusion method on Casitone agar (Bacto-Casitone, 9 g/liter; glucose, 20 g/liter; yeast extract, 5 g/liter; chloramphenicol, 0.5 g/liter; agar, 18 g/liter; pH 7.2) using Neosensitab tablets from Rosco Diagnostic (Taastrup, Denmark) as previously described (4, 5, 9). Determination of MICs was performed by the Etest procedure on Casitone agar plates according to the recommendations of the manufacturer (AB Biodisk, Solna, Sweden). All experiments were performed in triplicate, and results, which are expressed as mean values, were compared using the Wilcoxon-Mann-Whitney test.

Gene sequencing. Primers used for Cg*ERG4*, Cg*ERG5*, and Cg*ERG6* gene sequencing are presented in Table 1. They were designed with the WebPrimer program (http://seq.yeastgenome.org/cgi-bin/web-primer) from *C. glabrata* CBS138 Cg*ERG4*, Cg*ERG5*, and Cg*ERG6* gene sequences (GenBank accession numbers NC005967, NC006036, and NC006031, respectively) and synthesized by Eurogentec (Seraing, Belgium). The Cg*ERG11* gene was sequenced using primers previously designed in our laboratory (5). The sequencing products were prepared as previously described (38) and analyzed on a CEQ8000 DNA analysis system (Beckman Coulter, Inc., Fullerton, CA).

mRNA extraction and real-time reverse transcription-PCR. Total RNA was extracted from exponential-phase (24 h at 37°C) YEPD broth cultures as previously described (38) and used to quantify the expression of genes involved in drug efflux (Cg*CDR1* and Cg*CDR2*) or in ergosterol biosynthesis (Cg*ERG1*, Cg*ERG2*, Cg*ERG3*, Cg*ERG4*, Cg*ERG5*, Cg*ERG6*, Cg*ERG9*, and Cg*ERG11*). The mRNA level of Cg*STE12*, a gene coding a transcription factor involved in morphology switching in *C. glabrata* (6), was also quantified. Reverse transcription (RT) and real-time PCR were performed in triplicate as previously described (38), and standard deviations were calculated for each value. Primers used to perform real-time RT-PCR experiments are described in Table 1.

Other phenotype studies. Total sterols of the two clinical isolates were extracted as described before (5), and the amount of Δ5,7-dienols was evaluated by the maximum absorbance at 281.5 nm (33). The sterol species of the heptanic fraction were separated and analyzed by gas chromatography using an AT-1 capillary column (25 m by 0.32 mm; Alltech Canada Biotechnology Centre Inc., Guelph, Canada) as previously described (38).

The cell morphology of both isolates was studied microscopically from cultures grown for 48 h at 37°C on various agar-based media, all containing chloramphenicol (0.5 g/liter): YEPD agar, yeast extract-peptone-glycerol agar (yeast extract, 5 g/liter; peptone, 10 g/liter; glycerol, 20 g/liter; agar, 20 g/liter), Casitone agar, RPMI-glucose agar (RPMI 1640 from Sigma Aldrich, 10.4 g/liter; 3-[*N*-morpholino]-propanesulfonic acid hemisodium salt, 165 mM; L-glutamine, 2 mM; glucose, 20 g/liter; agar, 15 g/liter), Shadomy medium (yeast nitrogen base, 13.4 g/liter; glucose, 20 g/liter; L-asparagine, 1.5 g/liter; agar, 18 g/liter), rice extract agar-Tween medium (rice extract, 2.5 g/liter; Tween 80, 10 ml; agar, 20 g/liter), and malt agar (malt extract, 15 g/liter; agar, 15 g/liter). Ultrastructure was investigated by transmission electron microscopy performed as previously described (35) on blastoconidia from YEPD agar plates with a JEM-2010 transmission electron microscope (Jeol, Paris, France).

Susceptibility of isolate 21229 to Congo red and calcofluor white, two markers of the cell wall structure polysaccharides β-glucans and chitin, was evaluated in comparison with isolate 21231 by determining the minimum concentration of the dye that inhibited growth of the same quantity of cells for the two isolates. To visualize the cell wall structure polysaccharides, blastoconidia were labeled with calcofluor white by incubation for 30 min in a 10-μg/ml solution of the fluorescent dye and examined at 500 nm with an Olympus microscope equipped with epifluorescence.

For both isolates, growth curves were determined by monitoring the absorbance at 590 nm of three independent cultures in YEPD broth at 37°C for 30 h with constant shaking.

Complementation study. To verify the role of the Cg*ERG6* mutation in the decreased susceptibility to amphotericin B and in its pseudohyphal growth, a plasmid containing a wild-type copy of the Cg*ERG6* gene and derived from pRS416, a centromeric plasmid containing the *URA3* open reading frame (ORF) of *S. cerevisiae* which has been described to efficiently complement the uracil auxotrophy in *C. glabrata* (39), was used to transform a *ura3* derivative of the clinical isolate 21229. Briefly, a PCR fragment containing the wild-type *ERG6* ORF was obtained from *C. glabrata* isolate 21231 and cloned into pGEM-T (Promega, Madison, WI). After release from pGEM-T by digestion with the restriction endonucleases SacI and SacII (New England Biolabs, Ipswich, MA), the *ERG6* gene was cloned into pRS416 (LGC Promochem, Teddington, United Kingdom), and the obtained plasmid was named pRSERG628. A *ura3* derivative of the clinical isolate 21229 was selected on YEPD agar plates containing 1 g/liter 5-fluoroorotic acid. Inactivity of the *URA3* gene leading to uracil auxotrophy was verified by transformation of this mutant with pRS416. This *ura3* mutant, named 21229F34, was transformed with the pRSERG628 plasmid by following the procedure described for *S. cerevisiae ERG6* mutants (11). Two clones growing on selective medium were tested for amphotericin B susceptibility, and their morphology was studied by light microscopy as described above. Efficiency of the transformation was checked by plasmid extraction performed with the Zymoprep II kit (Zymoresearch, Orange, CA), followed by digestion of the plasmid by SacI and SacII.

Nucleotide sequence accession numbers. Sequences determined for Cg*ERG4*, Cg*ERG5*, Cg*ERG6*, and Cg*ERG11* for isolates 21231 and 21229 were deposited in the GenBank database and are available under accession numbers AY942649, AY942651, AY942653, DQ060157, AY942648, AY942650, AY942652, and AY942647, respectively (see Table 4).

TABLE 2. Susceptibility of *C. glabrata* isolates 21229 and 21231 to polyenes and azoles[a]

Antifungal	Diam (mm) of the inhibition zone with isolate:	
	21231	21229
Polyenes		
Amphotericin B	34	13
Nystatin	34	16
Azoles		
Miconazole	18	30
Clotrimazole	26 (M)	40
Ketoconazole	24 (M)	50
Fluconazole	20 (M)	50
Itraconazole	16	30
Voriconazole	36	43

[a] In vitro susceptibility testing was performed by a disk diffusion method on Casitone agar plates using Neosensitab tablets (containing 1 μg of drug for voriconazole, 8 μg for itraconazole, 10 μg for amphotericin B, econazole, miconazole, and clotrimazole, 15 μg for fluconazole and ketoconazole, and 50 μg for nystatin). Results, which are expressed as means of triplicate values, correspond to the diameter of growth inhibition zones. Standard deviations of the means represented less than 10% and mean diameters of growth inhibition zones were statistically different between the two isolates using the Wilcoxon-Mann-Whitney test at the unilateral risk of $\alpha = 0.05$. M, presence of resistant colonies in the growth inhibition zone.

RESULTS

Antifungal susceptibility. Antifungal susceptibility testing showed for isolate 21229 a lower susceptibility to polyenes associated with an increased susceptibility to azoles than for isolate 21231. By the disk diffusion method, large growth inhibition zones were seen on Casitone agar plates with both azoles and polyenes for isolate 21231, whereas they were small-sized with nystatin and amphotericin B and almost twofold larger with azoles for isolate 21229 (Table 2). These results were confirmed by determination of amphotericin B, ketoconazole, fluconazole, itraconazole, and voriconazole MICs performed by the Etest procedure on Casitone agar plates (Table 3). The amphotericin B MIC for isolate 21229 was more than 40-fold higher than for isolate 21231 (1.3 and 0.029 μg/ml, respectively), whereas azoles MICs were on average 5-fold lower than those for isolate 21231. Conversely, no differences were seen between the two isolates regarding their susceptibility to caspofungin, which was not available as Neosensitab

TABLE 3. MICs of polyene, azole, and echinocandin drugs for *C. glabrata* isolates 21229 and 21231[a]

Antifungal	MIC (mg/ml) for isolate:	
	21231	21229
Amphotericin B	0.029	1.3
Ketoconazole	0.136	0.034
Fluconazole	3.7	1
Itraconazole	18.7	1.8
Voriconazole	0.125	0.047
Caspofungin	0.023	0.024

[a] Results are expressed as mean values of three independent determinations. Data were obtained by the E-test procedure using antifungal strips on Casitone agar plates. Mean MICs were statistically different between the two isolates using the Wilcoxon-Mann-Whitney test at the unilateral risk of $\alpha = 0.05$, except for caspofungin.

tablets and therefore evaluated only by the Etest procedure (Table 3).

Sterol composition. Chromatographic analysis of the sterol molecular species revealed severe changes in the sterol composition of polyene-resistant isolate 21229. Indeed, whereas ergosterol was the major sterol species in wild-type isolate 21231, this sterol was not detectable in isolate 21229 (Fig. 1). By contrast, numerous sterol intermediates which could not be identified precisely accumulated in cells of isolate 21229. However, quantitative analysis which is based on the strong absorbance of UV light at 281.5 nm caused by ergosterol and the other Δ5,7-dienols (containing two conjugated double bonds in C-5 and C-7), revealed no differences between the two isolates (data not shown). Therefore, sterol intermediates detected in cells of isolate 21229, were considered non-ergosterol Δ5,7-dienols.

Analysis of Cg*ERG4*, Cg*ERG5*, Cg*ERG6*, and Cg*ERG11* gene sequences. As illustrated in Table 4, some point mutations were found in Cg*ERG4*, Cg*ERG5*, Cg*ERG6*, and Cg*ERG11* gene sequences for isolates 21231 and 21229 compared with the corresponding sequences from strain CBS 138 available in the GenBank database. Among polymorphisms detected inside or outside the coding sequences, some nucleotide substitutions were shared by the two clinical isolates, whereas others were found only in one isolate or the other. For Cg*ERG4*, Cg*ERG5*, and Cg*ERG11*, no mutation detected inside coding sequences had consequences

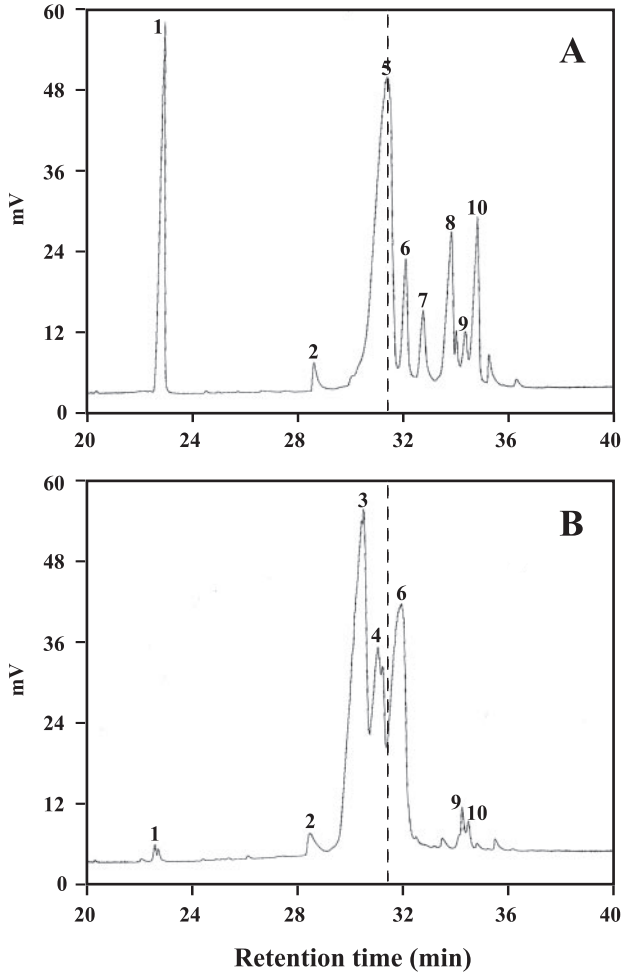

(C): Percentages of ergosterol biosynthesis intermediates in *C. glabrata* isolates 21231 and 21229.

Peak number[a]	Isolate	
	21231	21229
1	18.2	0.7
2	1.1	1.2
3	ND*	22.7
4	ND*	20.1
5	52.2	ND*
6	5.3	30.9
7	3.8	ND*
8	10.4	ND*
9	1.7	1.2
10	8.4	1.1

*Not detected.
[a]Peak numbers refer to panels A and B.

FIG. 1. Variations in sterol profiles of *C. glabrata* isolates 21231 and 21229. Sterols of the heptanic fraction were analyzed by gas chromatography. As highlighted by the dashed line, ergosterol, which was the major sterol species for isolate 21231 (A), was not detectable on the chromatogram of isolate 21229 (B). (C) Percentages of the ergosterol biosynthesis intermediates determined from the corresponding peak areas and retention times.

TABLE 4. Mutations detected in Cg*ERG4*, Cg*ERG5*, Cg*ERG6*, and Cg*ERG11* genes for *C. glabrata* isolates 21231 and 21229

Isolate	Accession no. and point mutations for gene[a]:			
	Cg*ERG4*	Cg*ERG5*	Cg*ERG6*	Cg*ERG11*
21231	AY942649; A-429T,[b] T-322C,[b] **T842A**, **T947C**,[b] G1490A	AY942651; A-373G,[b] G-367X,[b] G-314A, T-35C,[b] X-34A, C-33T, A-32T, C-27T	AY942653; G-268A,[b] A-209X,[b] **A524G**,[b] **G1064A**, C1196T[b]	DQ060157; **T767C**,[b] **C836T**, **A1022G**,[b] **T1556A**[b]
21229	AY942648; A-429T,[b] T-322C,[b] **T947C**,[b] **G1394A**	AY942650; A-373G,[b] G-367X,[b] A-311G, T-36A, T-35C,[b] C-33X, C-31T, **C426T**, **A1156G**	AY942652; G-268A,[b] A-209X,[b] C-199G, T-136A, **T515C**, **A524G**,[b] **G592T**, C1196T[b]	AY942647; **C677T**, **T767C**,[b] **A1022G**,[b] **T1274C**, **T1520A**, **T1556A**[b]

[a] Mutations are described as follows. The first letter corresponds to the nucleotide present in the GenBank database sequence for the corresponding gene (accession numbers NC005967, NC006036, NC006031, and L40389 for Cg*ERG4*, Cg*ERG5*, Cg*ERG6*, and Cg*ERG11*, respectively), the number represents the relative position from the start of the ORF, and the second letter represents the nucleotide found in the *ERG* gene sequence of isolate 21231 or 21229. Mutations located inside the coding sequences are in boldface type, and the missense mutation found in the isolate 21229 Cg*ERG6* gene sequence is underlined. Other mutations correspond to polymorphisms outside the coding sequences. The letter X placed after the number indicates a deletion of the corresponding nucleotide, and the same letter placed before the number corresponds to an insertion.

[b] Mutations shared by isolates 21231 and 21229.

on the amino acid sequence of the corresponding protein. In addition, silent mutations in the Cg*ERG6* gene sequence were detected for both isolates, but a missense mutation was also seen for polyene-resistant isolate 21229, i.e., replacement of a guanine with a thymine at position 592, leading to the replacement of a cysteine with a phenylalanine at position 198 in the sequence of Δ(24) sterol C-methyltransferase. All sequences were deposited in GenBank database and are available under the accession numbers indicated in Table 4.

Expression levels of genes potentially involved in the unusual phenotype of isolate 21229. Isolate 21229 displayed overexpression of genes coding for ABC transporters by real-time RT-PCR. Indeed, the Cg*CDR1* mRNA level in cells of this isolate was 27.2-fold higher than that for the control isolate, and the relative increase was 17.8 for the Cg*CDR2* gene (Fig. 2). Real-time RT-PCR experiments also revealed that all genes encoding enzymes involved in late steps of the ergosterol biosynthesis pathway (after 14α demethylation) and Cg*ERG11* itself were overexpressed in isolate 21229, compared to isolate 21231, with relative increases ranging from 13.4 to 43.3. Conversely, no real differences were observed between the two isolates regarding the expression of some genes encoding enzymes involved in early steps of this biosynthesis pathway, Cg*ERG1* and Cg*ERG9*. Likewise, no differences were seen between the two isolates in the expression level of the Cg*STE12* gene.

Cell morphology. Microscopic observation of cells of the isolate 21229 grown on different culture media revealed pseudohyphal growth regardless of the culture medium used. As illustrated in Fig. 3, cells of this isolate were arranged in small chains, sometimes branched. Daughter cells, which remained attached to the mother cells, emitted one or two buds at the opposite pole, a characteristic of pseudohyphae. In contrast, isolate 21231 presented the morphology classically described for *C. glabrata*, with round cells, sometimes budding.

Transmission electron microscopy confirmed these observations. As shown in Fig. 4, mother cells bearing up to three daughter cells of similar size were seen for isolate 21229, confirming its pseudohyphal growth. Moreover, the inner layer of the cell wall appeared thinner for this isolate than for control cells (Fig. 4B), suggesting changes in biosynthesis of its components or in their assembly.

Susceptibility to calcofluor white and Congo red. Susceptibility of the two isolates to markers of the main cell wall polysaccharides was also investigated. The growth of the two isolates was not inhibited by the presence of Congo red in the culture medium, even at the highest concentration used of 4 mg/ml. Conversely, growth of isolate 21229 was inhibited at the lowest concentration of calcofluor white, 0.1 mg/ml (Fig. 5B), whereas a concentration of 2 mg/ml of calcofluor white was required to inhibit growth of isolate 21231 (Fig. 5A).

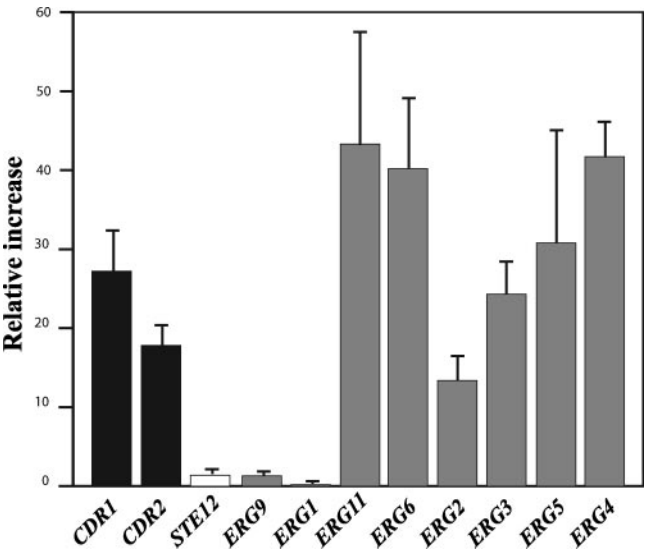

FIG. 2. Gene expression level in isolate 21229 compared with isolate 21231. The expression levels of genes coding for ABC transporter (Cg*CDR1* and Cg*CDR2*; black bars), a MAP-activated transcription factor involved in pseudohyphal growth (*STE12*; white bar), or enzymes involved in ergosterol biosynthesis (*ERG1*, *ERG2*, *ERG3*, *ERG4*, *ERG5*, *ERG6*, *ERG9*, *ERG11*; gray bars) were determined by RT-PCR. The relative increase (RI) in expression of the studied genes in isolate 21229 was determined as follows: $RI = 2\ \exp[(C_t \text{ gene} - C_t \text{ actin})_{\text{isolate 21229}} - (C_t \text{ gene} - C_t \text{ actin})_{\text{isolate 21231}}]$. C_t (cycle threshold) is defined as the number of cycles for which the curve representing the fluorescence intensity according to the number of cycles cuts a baseline arbitrarily defined as one fluorescence unit. Results correspond to mean values of results from three independent experiments (±standard deviation).

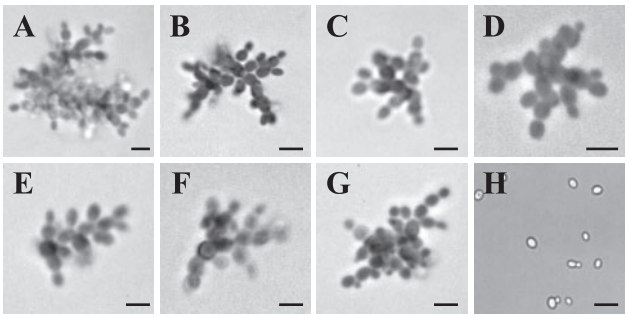

FIG. 3. Morphology of *C. glabrata* isolate 21229 on different agar-based culture media: Shadomy (A), YEPD (B), yeast extract-peptone-glycerol (C), RPMI-glucose (D), rice cream-Tween 80 (E), malt (F), and Casitone (G). Fungal cells were suspended in lactic blue dye, mounted on glass slides, and examined by light microscopy. A pseudohyphal growth was seen for isolate 21229 regardless of the culture medium. (H) Isolate 21231 grown on YEPD agar showing solitary blastoconidia and some budding cells. Bars, 20 μm.

Considering these results, cells of the two isolates were examined by fluorescence microscopy after staining with calcofluor white. The entire periphery was labeled for control cells, as well as septa between mother and daughter cells. Conversely, calcofluor white mainly bound to septa for cells of isolate 21229, whose periphery was slightly labeled (data not shown).

Consequences of the *ERG6* gene mutation on growth capacity. Polyene-resistant isolate 21229 presented a decreased growth rate compared with wild-type isolate 21231 (Fig. 6). If the latency period remained almost unmodified, the generation time during the exponential growth phase of isolate 21229 was of 10 h, whereas it was only 1 h for isolate 21231. Likewise, the maximum absorbance reached by the resistant clinical isolate was about twofold lower than the susceptible one.

Phenotype of a complemented *ura3* derivative of the clinical isolate 21229. As illustrated in Fig. 7, the disk diffusion method showed for clinical isolate 21229 and its *ura3* derivative 21229F34 a poor susceptibility to amphotericin B, with growth inhibition zones of 16 mm in diameter, whereas the complemented strain, named 21229C218, was susceptible to this drug (inhibition zone of 30 mm). Likewise, cells of the strain bearing the *ERG6*-containing plasmid presented a classical morphology for *C. glabrata* (Fig. 7F), with solitary round cells, sometimes budding, whereas the clinical isolate and its *ura3* derivative grew as pseudohyphae (Fig. 7D and E).

DISCUSSION

Polyene resistance, with few exceptions (e.g., *Candida dubliniensis* and *C. lusitaniae*), remains extremely rare in clinical isolates of pathogenic yeasts, although cases involving isolates resistant to this class of antifungal have been increasingly reported during the past two decades. Moreover, it has never been described as yet in clinical isolates of *C. glabrata*. Here, we studied a clinical isolate of *C. glabrata* presenting at first isolation a poor susceptibility to polyenes and a pseudohyphal growth.

Standard procedures of antifungal susceptibility testing demonstrated that the 21229 isolate had reduced susceptibility to polyenes and an increased susceptibility to azoles. This may appear somewhat surprising, since polyene resistance is often associated with resistance to azoles. In *S. cerevisiae*, deletion of *ERG3* leads to resistance to both azoles and nystatin (40). Likewise, for *C. albicans*, null mutants for *ERG11*, which can be selected by culture on amphotericin B-containing medium,

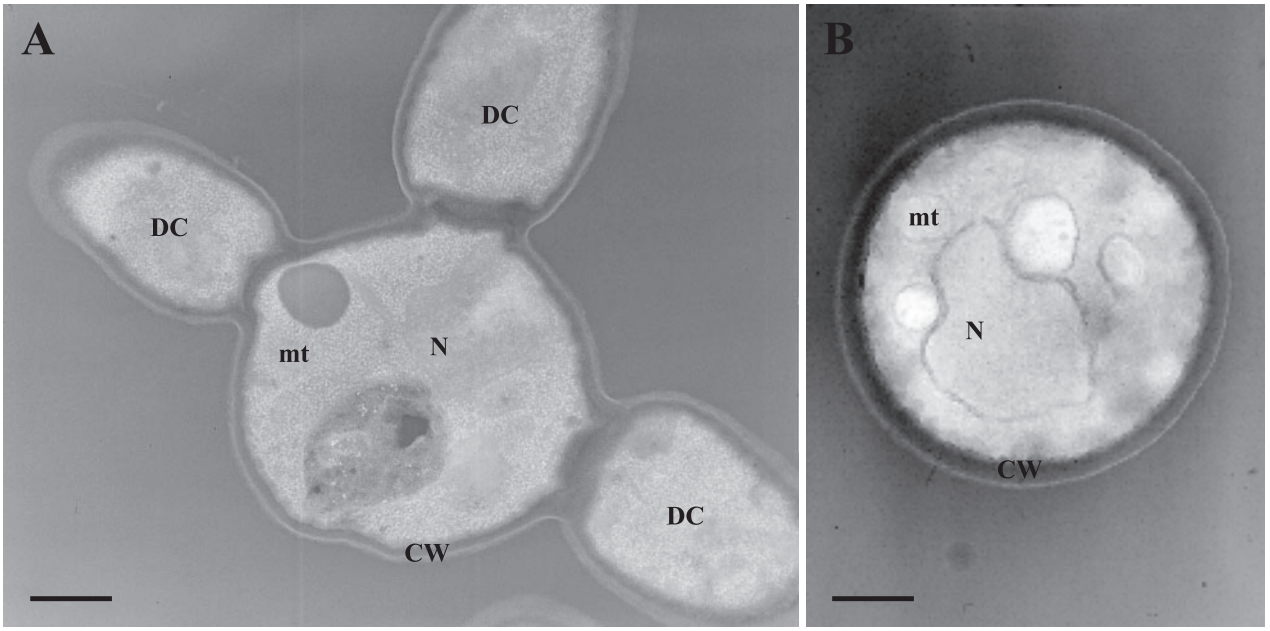

FIG. 4. Transmission electron micrographs of *C. glabrata* isolates 21229 (A) and 21231 (B). Transmission electron microscopy confirmed the pseudohyphal growth of isolate 21229, with cells presenting up to three daughter cells of similar size, and revealed the ultrastructural changes of their cell wall with a thinner inner layer compared with cells of control isolate. N, nucleus; mt, mitochondrion; CW, cell wall; DC, daughter cell.

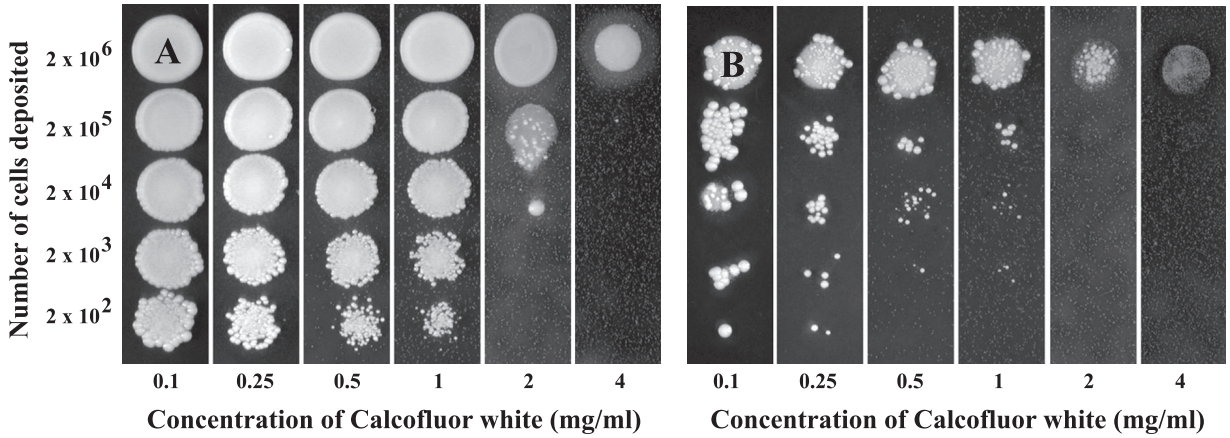

FIG. 5. Susceptibility of *C. glabrata* isolates 21231 (A) and 21229 (B) to calcofluor white. Susceptibility was evaluated by inoculation of various quantities of cells (from 2×10^6 to 2×10^2) on YEPD agar plates containing increasing concentrations of the dye (from 0.1 to 4 mg/ml). Calcofluor white inhibited the growth of isolate 21229 at a concentration as low as 0.1 mg/ml, whereas a concentration of 2 mg/ml was required to inhibit the growth of isolate 21231.

are also resistant to azoles (28). Moreover, previous works from Kelly et al. (15) and Nolte et al. (22) reported the isolation and characterization of clinical azole- and amphotericin B-resistant *C. albicans* isolates from AIDS or leukemic patients. Likewise, association of resistance to polyenes and azoles have also been demonstrated in laboratory-induced mutants of *C. albicans* (3). However, azole resistance is not systematically associated with an altered susceptibility to polyenes, as demonstrated in *C. albicans* mutants by Niimi et al. (20), and conversely, *erg1* mutants of *C. glabrata* present an increased susceptibility to azoles and are resistant to nystatin (36).

The ergosterol biosynthesis pathway, essentially studied in *S. cerevisiae* (24, 25), is a complex metabolic pathway. More than 20 enzymes and the genes that encode them are known today in this yeast. Although a standard order has been described, different enzymes may act on a same substrate, which increases markedly the number of potential sterol intermediates. Moreover, as demonstrated by the systematic deletion of the *S. cerevisiae* open reading frames, some of these metabolic steps are crucial for cell viability. For example, *ERG7*, *ERG8*, *ERG9*,

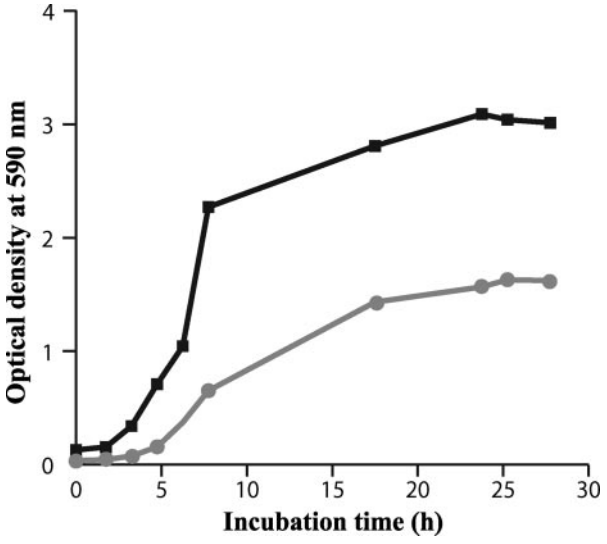

FIG. 6. Growth curves of *C. glabrata* isolates 21231 (black) and 21229 (gray). Growth curves were drawn by monitoring the absorbance at 590 nm of cultures in YEPD broth incubated at 37°C for 30 h. Results correspond to mean absorbances of three independent cultures. For each value, the standard deviation did not exceed 10%.

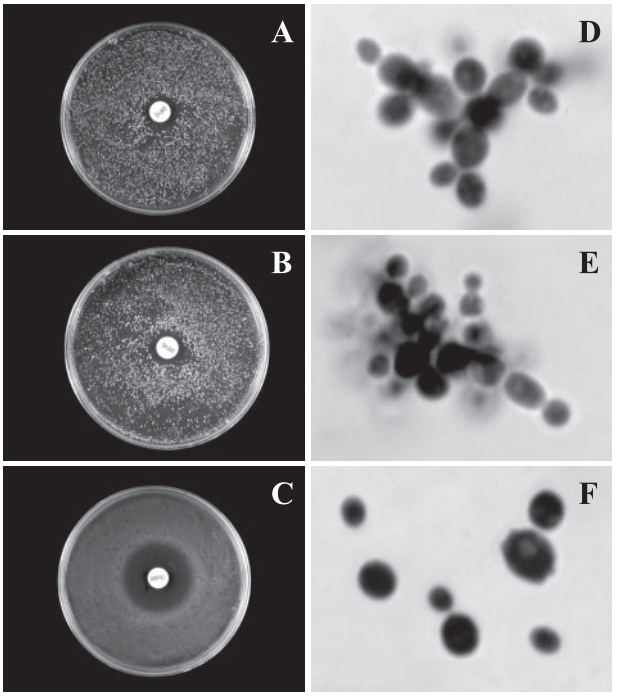

FIG. 7. Susceptibility to amphotericin B (A, B, and C) and microscopic morphology (D, E, and F) of the cells for *C. glabrata* isolate 21229 (A and D), its ura3 derivative 21229F34 (B and E), and the complemented strain 21229C218 (C and F). The complementation of isolate 21229 with a wild-type copy of the *ERG6* gene restored the susceptibility to amphotericin B as well as a classical morphology, consisting of solitary blastoconidia.

ERG10, *ERG11*, *ERG12*, *ERG19*, *ERG20*, *ERG25*, *ERG26*, and *ERG27* deletions are lethal. Conversely, invalidation of *ERG2* and *ER24* genes results in viable mutants with minor phenotypic alterations, e.g., moderate growth defect and ergosterol auxotrophy (2, 18, 19), whereas *ERG6* null mutants show defective conjugation and tryptophan uptake as well as a diminished capacity for transformation. In addition, *erg6* mutants grow as short chains of elongated cells and present a resistance to nystatin associated with a hypersensitivity to cycloheximide, anthracyclins, and brefeldin A (11, 12, 14). Likewise, inactivation of the *ERG3* gene in *S. cerevisiae* results in changes in the susceptibility to ketoconazole (40), syringomycin (34), and nalidixic acid (27), and *ERG3* null mutants are unable to grow on nonfermentable carbon sources and are cold sensitive (1, 13, 32).

Since ergosterol is the polyene target, a qualitative and quantitative analysis of sterols was performed. Results from gas chromatography indicated a lack of ergosterol in our polyene-resistant clinical isolate, offset by the accumulation of sterol intermediates identified as Δ5,7-dienols on the basis of their strong absorbance at 281.5 nm. These changes in sterol content suggest a mutation in genes encoding enzymes involved in late steps of the ergosterol pathway, as usually reported previously (10, 26).

Ergosterol itself and the other Δ5,7-dienols are characterized by the presence of two conjugated double bonds in C-5 and C-7, resulting from the activity of *ERG3* gene product, C-5 sterol desaturase (1). Considering the detection of non-ergosterol Δ5,7-dienols in isolate 21229, one may speculate a functional C-5 sterol desaturase and the inactivation of one of the last two enzymes of the ergosterol biosynthesis pathway. However, gene sequencing revealed that C-24 sterol reductase (CgERG4p) and C-22 sterol desaturase (CgERG5p) were not modified. Nevertheless, it is well established that a same enzyme may intervene at different levels of the ergosterol biosynthesis pathway (28). Moreover, previous works demonstrated that an *ERG6* mutation may also cause polyene resistance (11, 42). In the current study, a missense mutation in the Cg*ERG6* gene for isolate 21229 led to a predicted C→F substitution (C198F) in the corresponding protein. Even without the crystal structure of the C-24 methyltransferase, such a nonconservative change might be expected to lead to major changes in enzyme structure and activity.

The ergosterol biosynthesis pathway was further investigated by quantification of gene expression by real-time RT-PCR. In wild-type strains of *S. cerevisiae*, a negative feedback is exercised by ergosterol upon its own biosynthesis from the demethylation step, and the only modification of the side chain is sufficient to disturb this negative feedback (7, 30). For example, disruption of genes encoding enzymes involved in late steps of the ergosterol biosynthesis pathway increased expression of *ERG5*, *ERG6*, and *ERG24* genes (33). In isolate 21229, an induction of the ergosterol biosynthesis pathway was also seen, since all genes encoding enzymes usually involved after demethylation and Cg*ERG11* itself were overexpressed. This overexpression of Cg*ERG11*, which is well known as one of the mechanisms of azole resistance (41), may appear to conflict with the increased susceptibility of isolate 21229 to azoles. In our strain, which seems unable to produce enough ergosterol to supply growth, induction of the sterol biosynthesis pathway may be an obligate adaptation to provide a sufficient amount of non-ergosterol Δ5,7-dienols to maintain cell viability. However, accumulation of these intermediates, which cannot absolutely replace ergosterol functionally, therefore renders the isolate 21229 more sensitive to azole drugs, as observed in our experiments. Another observation which seems to be inconsistent with the increased susceptibility to azoles is the overexpression of Cg*CDR1* and Cg*CDR2* genes revealed by real-time RT-PCR. This increased mRNA level of genes encoding efflux pumps could also be related to the accumulation of non-ergosterol Δ5,7-dienols. The ABC proteins CgCDR1p and CgCDR2p would be overexpressed to eliminate these abnormal sterol intermediates. Alternatively, one may speculate that lack of ergosterol in our clinical isolate 21229 could also disturb protein trafficking and especially prevent CgCDR1p and CgCDR2p targeting to the plasma membrane. Indeed, alterations of protein trafficking due to modifications of membrane sterol composition have been described for *S. cerevisiae*, which is closely related to *C. glabrata* (37). Thus, the decreased efflux capacity of cells of isolate 21229 would explain their higher susceptibility to azole drugs despite Cg*ERG11* overexpression.

Neither hyphae or pseudohyphae are produced by *C. glabrata*, except under special culture conditions like nitrogen starvation or in the presence of $CuSO_4$, which lead, through a mitogen-activated protein (MAP) kinase signaling cascade, to the activation of *STE12*, a transcription factor necessary for morphology switching (8, 17). However, pseudohyphal growth of isolate 21229 was not dependent on the culture medium, and no overexpression of *STE12* was seen. Transmission electron microscopy confirmed the pseudohyphal growth of isolate 21229 and revealed a structural modification of the cell wall with a thinner inner layer which was associated with a growth defect, as revealed by growth kinetic experiments. These observations are consistent with the greater susceptibility of the growing cells of this isolate to calcofluor white and with the poor staining of mutant cells by this dye, which suggested modifications of the distribution or composition of the cell wall polysaccharides. All of these phenotypic changes may be related to perturbations of protein trafficking and, for instance, to alterations of the targeting to the plasma membrane of enzymes involved in cell wall polysaccharide synthesis (i.e., β-glucan synthase) or degradation (i.e., glucanase). However, the increased susceptibility of cells of isolate 21229 to calcofluor white may also arise from an increase in the chitin content in response to cell wall stress.

In conclusion, we describe here a clinical isolate of *C. glabrata* in which a unique molecular event was responsible for several phenotypic changes. Indeed, the missense mutation that we detected in the Cg*ERG6* gene lead, by the inactivation of C-24 sterol methyltransferase, to the interruption of the ergosterol biosynthesis pathway and, therefore, to polyene resistance. As confirmed by complementation studies, the changes in sterol composition of the plasma membrane induced by this mutation are also responsible for the pseudohyphal growth, probably through alterations of the targeting of some proteins required for daughter cell liberation to the plasma membrane. Two other observations confirming this putative mistargeting to the plasma membrane are the high susceptibility of the clinical isolate to azole drugs and to calcofluor white, which might be related to changes in the trafficking of the efflux

pumps (whenever overexpressed) and β-glucan synthase and/or chitin synthase to the plasma membrane, respectively. Determination of the subcellular localization of these enzymes, by construction of fusion proteins with green fluorescent protein, would confirm this last hypothesis.

ACKNOWLEDGMENTS

P.V. is a recipient of a grant from Angers Loire Metropole. This study was supported in part by a grant from the Institut de Parasitologie de l'Ouest, Rennes, France.

We thank Pascal Reynier (EMI-U00.18, Angers, France) and Alain Morel (INSERM U564, Angers, France) for their help in gene sequencing and in quantitative PCR analysis of gene expression.

REFERENCES

1. **Arthington, B. A., L. G. Bennett, P. L. Skatrud, C. J. Guynn, R. J. Barbuch, C. E. Ulbright, and M. Bard.** 1991. Cloning, disruption and sequence of the gene encoding yeast C-5 sterol desaturase. Gene **102:**39–44.
2. **Ashman, W. H., R. J. Barbuch, C. E. Ulbright, H. W. Jarrett, and M. Bard.** 1991. Cloning and disruption of the yeast C-8 sterol isomerase gene. Lipids **26:**628–632.
3. **Barker, K. S., S. Crisp, N. Wiederhold, R. E. Lewis, B. Bareither, J. Eckstein, R. Barbuch, M. Bard, and P. D. Rogers.** 2004. Genome-wide expression profiling reveals genes associated with amphotericin B and fluconazole resistance in experimentally induced antifungal resistant isolates of *Candida albicans*. J. Antimicrob. Chemother. **54:**376–385.
4. **Brun, S., C. Aubry, O. Lima, R. Filmon, T. Bergès, D. Chabasse, and J. P. Bouchara.** 2003. Relationships between respiration and susceptibility to azole antifungals in *Candida glabrata*. Antimicrob. Agents Chemother. **47:**847–853.
5. **Brun, S., T. Bergès, P. Poupard, C. Vauzelle-Moreau, G. Renier, D. Chabasse, and J. P. Bouchara.** 2004. Mechanisms of azole resistance in petite mutants of *Candida glabrata*. Antimicrob. Agents Chemother. **48:** 1788–1796.
6. **Calcagno, A. M., E. Bignell, P. Warn, M. D. Jones, D. W. Denning, F. A. Muhlschlegel, T. R. Rogers, and K. Haynes.** 2003. *Candida glabrata STE12* is required for wild-type levels of virulence and nitrogen starvation induced filamentation. Mol. Microbiol. **50:**1309–1318.
7. **Casey, W. M., J. P. Burgess, and L. W. Parks.** 1991. Effect of sterol side-chain structure on the feed-back control of sterol biosynthesis in yeast. Biochim. Biophys. Acta **1081:**279–284.
8. **Csank, C., and K. Haynes.** 2000. *Candida glabrata* displays pseudohyphal growth. FEMS Microbiol. Lett. **189:**115–120.
9. **Defontaine, A., J. P. Bouchara, P. Declerk, C. Planchenault, D. Chabasse, and J. N. Hallet.** 1999. In-vitro resistance to azoles associated with mitochondrial DNA deficiency in *Candida glabrata*. J. Med. Microbiol. **48:**663–670.
10. **Ellis, D.** 2002. Amphotericin B: spectrum and resistance. J. Antimicrob. Chemother. **49**(Suppl. 1)**:**7–10.
11. **Gaber, R. F., D. M. Copple, B. K. Kennedy, M. Vidal, and M. Bard.** 1989. The yeast gene *ERG6* is required for normal membrane function but is not essential for biosynthesis of the cell-cycle-sparking sterol. Mol. Cell. Biol. **9:**3447–3456.
12. **Graham, T. R., P. A. Scott, and S. D. Emr.** 1993. Brefeldin A reversibly blocks early but not late protein transport steps in the yeast secretory pathway. EMBO J. **12:**869–877.
13. **Hemmi, K., C. Julmanop, D. Hirata, E. Tsuchiya, J. Y. Takemoto, and T. Miyakawa.** 1995. The physiological roles of membrane ergosterol as revealed by the phenotypes of *syr1*/*erg3* null mutant of *Saccharomyces cerevisiae*. Biosci. Biotechnol. Biochem. **3:**482–486.
14. **Jensen-Pergakes, K. L., M. A. Kennedy, N. D. Lees, R. Barbuch, C. Koegel, and M. Bard.** 1998. Sequencing, disruption, and characterization of the *Candida albicans* sterol methyltransferase (ERG6) gene: drug susceptibility studies in erg6 mutants. Antimicrob. Agents Chemother. **42:**1160–1167.
15. **Kelly, S. L., D. C. Lamb, D. E. Kelly, N. J. Manning, J. Loeffler, H. Hebart, U. Schumacher, and H. Einsele.** 1997. Resistance to fluconazole and cross-resistance to amphotericin B in *Candida albicans* from AIDS patients caused by defective delat 5,6-desaturation. FEBS Lett. **400:**80–82.
16. **Krcmery, V., and A. J. Barnes.** 2002. Non-*albicans Candida* spp. causing fungaemia: pathogenicity and antifungal resistance. J. Hosp. Infect. **50:**243–260.
17. **Lachke, S. A., S. Joly, K. Daniels, and D. R. Soll.** 2002. Phenotypic switching and filamentation in *Candida glabrata*. Microbiology **148:**2661–7264.
18. **Lees, N. D., B. Skaggs, D. R. Kirsch, and M. Bard.** 1995. Cloning of the late genes in the ergosterol biosynthetic pathway of *Saccharomyces cerevisiae*—a review. Lipids **30:**221–2266.
19. **Lorenz, R. T., and L. W. Parks.** 1992. Cloning, sequencing, and disruption of the gene encoding sterol C-14 reductase in *Saccharomyces cerevisiae*. DNA Cell Biol. **11:**685–692.
20. **Niimi, M., K. Niimi, Y. Takano, A. R. Holmes, F. J. Fischer, Y. Uehara, and R. D. Cannon.** 2004. Regulated overexpression of *CDR1* in *Candida albicans* confers multidrug resistance. J. Antimicrob. Chemother. **6:**999–1006.
21. **Nissapatorn, V., C. Lee, Q. K. Fatt, and K. A. Abdullah.** 2003. AIDS-related opportunistic infections in Hospital Kuala Lumpur. Jpn. J. Infect. Dis. **56:** 187–192.
22. **Nolte, F. S., T. Parkinson, D. J. Falconer, S. Dix, J. Williams, C. Gilmore, R. Geller, and J. R. Wingard.** 1997. Isolation and characterization of fluconazole- and amphotericin B-resistant *Candida albicans* from blood of two patients with leukemia. Antimicrob. Agents Chemother. **41:**196–199.
23. **Odds, F. C., M. G. Rinaldi, C. R. Cooper, Jr., A. Fothergill, L. Pasarell, and M. R. McGinnis.** 1997. *Candida* and *Torulopsis*: a blinded evaluation of use of pseudohypha formation as basis for identification of medically important yeasts. J. Clin. Microbiol. **35:**313–316.
24. **Paltauf, F., S. Kohlwein, and S. A. Henry.** 1992. Regulation and compartmentalization of lipid synthesis in yeast, p. 415–500. *In* E. W. Jones, J. R. Pringle, and J. R. Broach (ed.), The molecular and cellular biology of the yeast *Saccharomyces*: gene expression. Cold Spring Harbor Laboratory Press, Cold Spring Harbor, NY.
25. **Parks, L. W., and W. M. Casey.** 1995. Physiological implications of sterol biosynthesis in yeast. Annu. Rev. Microbiol. **49:**95–116.
26. **Perea, S., and T. F. Patterson.** 2002. Antifungal resistance in pathogenic fungi. Clin. Infect. Dis. **35:**1073–1080.
27. **Prendergast, J. A., R. A. Singer, N. Rowley, A. Rowley, G. C. Johnston, M. Danos, B. Kennedy, and R. F. Gaber.** 1995. Mutations sensitizing yeast cells to the start inhibitor nalidixic acid. Yeast **6:**537–547.
28. **Sanglard, D., F. Ischer, T. Parkinson, D. Falconer, and J. Bille.** 2003. *Candida albicans* mutations in the ergosterol biosynthetic pathway and resistance to several antifungal agents. Antimicrob. Agents Chemother. **47:** 2404–2412.
29. **Sanglard, D., and F. C. Odds.** 2002. Resistance of *Candida* species to antifungal agents: molecular mechanisms and clinical consequences. Lancet Infect. Dis. **2:**73–85.
30. **Servouse, M., and F. Karst.** 1986. Regulation of early enzymes of ergosterol biosynthesis in *Saccharomyces cerevisiae*. Biochem. J. **240:**541–547.
31. **Singh, A., I. Bairy, and P. G. Shivananda.** 2003. Spectrum of opportunistic infections in AIDS cases. Indian J. Med. Sci. **57:**16–21.
32. **Smith, S. J., and L. W. Parks.** 1993. The *ERG3* gene in *Saccharomyces cerevisiae* is required for the utilization of respiratory substrates and in heme-deficient cells. Yeast **11:**1177–1187.
33. **Smith, S. J., J. H. Crowley, and L. W. Parks.** 1996. Transcriptional regulation by ergosterol in the yeast *Saccharomyces cerevisiae*. Mol. Cell Biol. **16:**5427–5432.
34. **Taguchi, N., Y. Takano, C. Julmanop, Y. Wang, S. Stock, J. Takemoto, and T. Miyakawa.** 1994. Identification and analysis of the *Saccharomyces cerevisiae SYR1* gene reveals that ergosterol is involved in the action of syringomycin. Microbiology **2:**353–359.
35. **Tronchin, G., J. P. Bouchara, R. Robert, and J. M. Senet.** 1988. Adherence of *Candida albicans* germ tubes to plastic: ultrastructural and molecular studies of fibrillar adhesins. Infect. Immun. **56:**1987–1993.
36. **Tsai, H. F., M. Bard, K. Izumikawa, A. A. Krol, A. M. Sturm, N. T. Culbertson, C. A. Pierson, and J. E. Bennett.** 2004. *Candida glabrata erg1* mutant with increased sensitivity to azoles and to low oxygen tension. Antimicrob. Agents Chemother. **48:**2483–2489.
37. **Umebayashi, K., and A. Nakano.** 2003. Ergosterol is required for targeting of tryptophan permease to the yeast plasma membrane. J. Cell Biol. **161:**1117–1131.
38. **Vandeputte, P., G. Larcher, T. Bergès, G. Renier, D. Chabasse, and J. P. Bouchara.** 2005. Mechanisms of azole resistance in a clinical isolate of *Candida tropicalis*. Antimicrob. Agents Chemother. **11:**4608–4615.
39. **Vermitsky, J. P., K. D. Earhart, W. L. Smith, R. Homayouni, T. D. Edlind, and P. D. Rogers.** 2006. *Pdr1* regulates multidrug resistance in *Candida glabrata*: gene disruption and genome-wide expression studies. Mol. Microbiol. **61:**704–722.
40. **Watson, P. F., M. E. Rose, and S. L. Kelly.** 1998. Isolation and analysis of ketoconazole resistant mutants of *Saccharomyces cerevisiae*. J. Med. Vet. Mycol. **3:**153–162.
41. **White, T. C., K. A. Marr, and R. A. Bowden.** 1998. Clinical, cellular, and molecular factors that contribute to antifungal drug resistance. Clin. Microbiol. Rev. **11:**382–402.
42. **Young, L. Y., C. M. Hull, and J. Heitman.** 2003. Disruption of ergosterol biosynthesis confers resistance to amphotericin B in *Candida lusitaniae*. Antimicrob. Agents Chemother. **47:**2717–2724.